

45 Performance Modeling Workshop hosted by Sandia National Lab (Stein and Farnung, 2017).
 46 Sandia National Laboratory has been promoting a collaborative framework for improving the
 47 accuracy of PV performance models, denoted as PVP MC (PV Performance Modeling
 48 Collaborative, <https://pvpmc.sandia.gov/>). Under this framework workshops and meetings are
 49 regularly organized, and tools and resources are freely offered as well. The PV LIB tool is a
 50 good example of a collection of functions for modeling PV performance that is gaining visibility
 51 and users (Andrews et al., 2014; Holmgren et al., 2015).

52
 53 The working of a solar cell is completely characterized by the relationship between the current
 54 generated and the voltage applied, denoted as the I-V characteristic curve. In modeling the
 55 behavior of PV cells, modules or arrays there are generally three main kinds of model
 56 approaches: the equivalent circuit diode models, the semi-empirical models and the simple
 57 efficiency approach. The equivalent circuit diode models consist of representing the PV
 58 generator with a diode equivalent circuit and solving the current-voltage characteristic
 59 equation; this is the case of the California Electrical Commission Model (De Soto et al., 2004;
 60 Dobos, 2012). The semi-empirical models use empirical correlations to extrapolate the specific
 61 points of the I-V curve to other temperature and irradiance conditions. Sandia Array
 62 Performance Model (SAPM) is the best known example of semi-empirical model (King et al.,
 63 2016, 2004; Peng et al., 2015). PVWatts is the most exponent of the third group of models
 64 (Dobos, 2014). Several assessment and comparison works on the performance of the different
 65 kind of models can be found elsewhere (Gurupira and Rix, 2017; Stein et al., 2013).

66
 67 The diode equivalent circuit model, single or double diode versions, has been used extensively
 68 in the literature (Celik and Acikgoz, 2007; Ciulla et al., 2014; Khezzer et al., 2014; Mares et al.,
 69 2015a; Nassar-Eddine et al., 2016; Rhouma et al., 2017). In this work an iterative method
 70 combined with the Lambert W-function is presented for solving the five parameters in the
 71 single diode equation method. The Lambert W-function is defined as the function that solves
 72 the equation

$$73 \quad W e^W = z \quad (1)$$

74
 75 where z is a complex number. The Lambert W-function has been extensively applied not only
 76 in PV modeling but also in other problems in physics and computer science (Valluri et al., 2000;
 77 Veberič, 2012). Solving delay differential equations, fracture growth dynamics and Wien's
 78 displacement law are a few examples of additional applications of Lambert W-function. Many
 79 other examples can be found elsewhere (Kazakova et al., 2010).

80
 81
 82 The methodology is used for the modeling of the I-V curves of PV modules of different
 83 technologies from the basic information provided in the manufacturer's datasheet. Even
 84 though the methodology is iterative, the approach presented in this paper is of fast
 85 convergence, robust and highly accurate. In addition, the I-V curves are modeled for different
 86 temperature and irradiance conditions both indoor and outdoor. The assessment of the
 87 methodology with experimental I-V curves at STC (Standard Test Conditions) and different
 88 temperature and irradiance conditions has shown good results. However, the sensitivity
 89 analysis also presented in this work evidenced that the accuracy of the methodology is
 90 partially conditioned by the uncertainty in the input parameters used by the model. Finally, the
 91 methodology showed robustness in extrapolating the curves beyond STC. The results
 92 demonstrated the equivalence between extrapolating the datasheet parameters to
 93 temperature and irradiance to solve afterwards the diode equation, and solving the diode
 94 equation at STC and extrapolating afterwards the five parameters to temperature and
 95 irradiance different conditions.

96

2. Methodology for computing the I-V curve

97
98
99

100 It is widely known that the behavior of a photovoltaic cell can be modeled with an equivalent
101 electrical circuit, frequently referred to as the diode equivalent circuit model (Green, 1981).
102 One of the most recognized approaches for diode equivalent circuits is the five parameter
103 model, which represents the PV cell by a circuit with one diode and two resistances (Fig 1). The
104 single-diode circuit equation for the five parameter model is (De Soto et al., 2006),
105

$$106 \quad I = I_L - I_0 \left[\exp\left(\frac{V+IR_s}{N_s a V_T}\right) - 1 \right] - \frac{V+IR_s}{R_{sh}} \quad (2)$$

107

108 where the aforementioned five parameters are: I_L is the photocurrent, I_0 is the reverse
109 saturation current of the diode, R_s is the series resistance, R_{sh} is the shunt resistance, and a is
110 the ideality factor of the diode. N_s is the number of series-connected cells in the module, and
111 V_T is:

$$112 \quad V_T = \frac{k T_{cell}}{q} \quad (3)$$

113

114

115

116

117

118

119

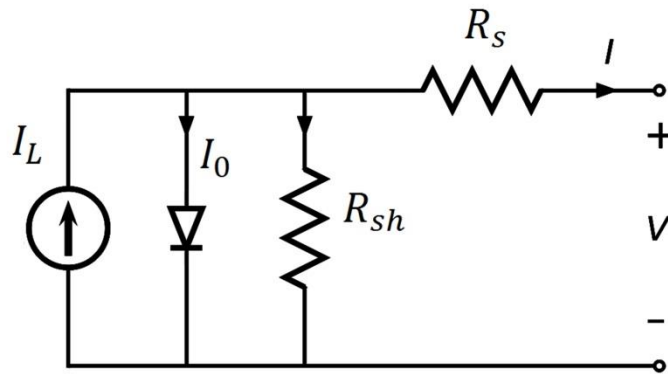
120

being T_{cell} the temperature of the cell, k is the Boltzmann's constant and q is the electron
charge.

121

122

123



124

125

126

Fig 1. Single-diode equivalent circuit of a solar cell.

127

128

129

130

131

132

133

134

135

136

137

138

139

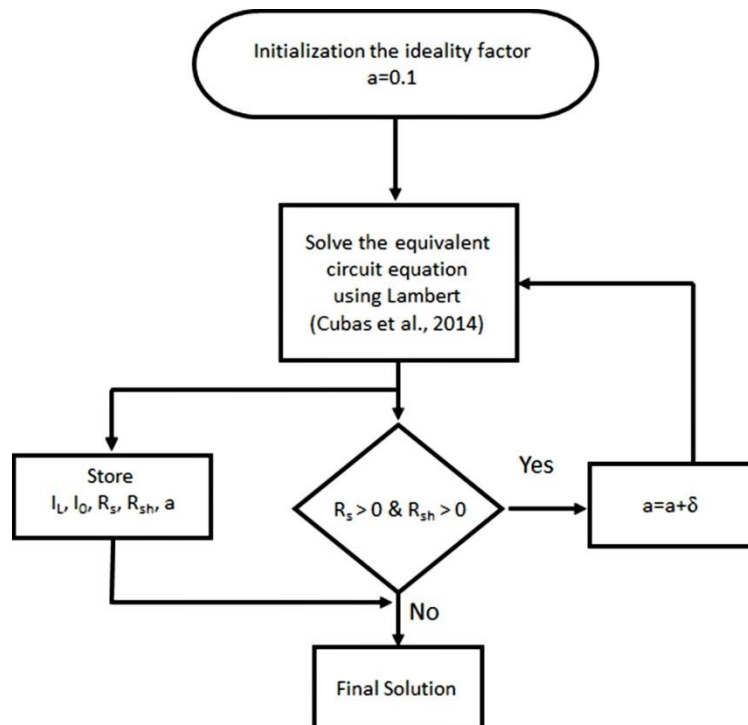
140

141

Equation (2) is a non-linear function of the current and voltage, and thus the solution is not straightforward and unique either. Different methods and approaches for solving the diode equation can be found elsewhere (Ayodele et al., 2016; Et-Torabi et al., 2017; Ghani et al., 2014; Mares et al., 2015b; Sudhakar Babu et al., 2016). In the case of having a prior estimation of the parameter a , it is possible to determine the other four parameters in a simple and straightforward way using the Lambert W-function by a set of equations recently proposed by Cubas et al. 2014 from the prior knowledge of the module's characteristic parameters (short-

133 circuit current I_{sc} , open-circuit voltage V_{oc} , and maximum power current and voltage I_{mp} and
 134 V_{mp}). This method proposes the use of the Lambert W-function to obtain the series resistance
 135 first and then computing the remaining three parameters from explicit equations that can be
 136 derived from the five parameter model (Cubas et al., 2014). This method presented a good
 137 response in modeling the five parameters at Standard Test Conditions (STC) for two multi and
 138 mono-crystalline silicon modules (Cubas et al., 2014). However, the methodology is limited by
 139 the fact of that it requires a previous knowledge of the ideality factor. In order to overcome
 140 this limitation, an interactive method on the ideality factor is proposed here for solving the five
 141 parameters of the diode equivalent circuit. The iteration runs on the ideality factor being
 142 increased by steps of $\delta=0.1$ as long as the resistances get positive values. The convergence
 143 criterion is reached when the series or the shunt resistance values resulting from solving the
 144 equations take a negative value, when the iteration stops and the last previous values of both
 145 resistances are taken as the best estimate ones. A similar convergence criteria applied only to
 146 the shunt resistance was recently proposed for extracting the value of the ideality factor
 147 (Rasool et al., 2017). This convergence criterion is very fast and the number of iterations was
 148 less than 50 in all the cases explored in this work. Figure 2 shows a flow diagram of the
 149 algorithm proposed here.

150
 151
 152



153
 154
 155
 156
 157
 158
 159

Fig 2. Flow diagram of the algorithm proposed for solving the diode equivalent circuit equation.

160
 161

Once the five parameters are determined, the I-V curve can be estimated by solving again the diode equation. For instance, the PV LIB tool (open source library of functions for modeling PV

162 systems released by Sandia National Lab) includes a procedure for computing the I-V curve by
 163 solving the diode equation using the Lambert W-function (Andrews et al., 2014; Holmgren et
 164 al., 2015; Jain, 2004).

165
 166 There are several formulations to describe the variations of the five parameters with
 167 irradiance and temperature as a function of the parameters at STC that can be used for
 168 extrapolating the I-V curve to outdoor conditions. The De Soto equations used in this work are
 169 (De Soto et al., 2006):

170

$$171 \quad I_L(G, T_{cell}) = \frac{G}{G_0} (I_{Lstc} + \alpha_{I_{sc}} (T_{cell} - T_{stc})) \quad (4)$$

172

173

$$174 \quad I_0(G, T_{cell}) = I_{0stc} \left[\frac{T_{cell}}{T_{stc}} \right]^3 \exp \left[\frac{1}{k} \left(\frac{E_g(T_{stc})}{T_{stc}} - \frac{E_g(T_{cell})}{T_{cell}} \right) \right] \quad (5)$$

175

176

177

$$178 \quad E_g(T_{cell}) = E_g(T_{stc}) (1 - \delta_{Eg} (T_{cell} - T_{stc})) \quad (6)$$

179

180

$$181 \quad R_{sh}(S) = R_{sh_stc} \left(\frac{G}{G_0} \right) \quad (7)$$

182

$$183 \quad a = a_{stc} \frac{T_{cell}}{T_{stc}} \quad (8)$$

184

185

186 Where G is the outdoor irradiance, G_0 is the irradiance at STC (1000 W m^{-2}), $\alpha_{I_{sc}}$ is the short-
 187 current temperature coefficient, T_{cell} is the cell temperature, T_{stc} is the reference
 188 temperature ($25 \text{ }^\circ\text{C}$), E_g is the energy band gap, δ_{Eg} the temperature dependence of the
 189 energy band gap, and the subscript stc denotes standard test conditions.

190

191 An additional approach to extrapolate the I-V curve to outdoor conditions is to calculate the
 192 variation of irradiance and temperature for the manufacturer parameters and use again the
 193 method proposed in Fig 2 for solving the diode equation and retrieving the five parameters.
 194 Thus, for the short circuit, open voltage and maximum power current and power the
 195 corrected parameters can be calculated by (De Soto et al., 2004; Kessaissia et al., 2015;
 196 Khezzer et al., 2014):

197

198

$$199 \quad I_{sc}^{corr} = I_{sc} \frac{G}{G_0} + \alpha_{I_{sc}} (T_{cell} - T_{stc}) \quad (9)$$

200

201

$$202 \quad V_{oc}^{corr} = V_{oc} + N_s a V_T \ln \left(\frac{G}{G_0} \right) + \beta_{V_{oc}} (T_{cell} - T_{stc}) \quad (10)$$

203

$$204 \quad I_{mp}^{corr} = I_{mp} \frac{G}{G_0} + \alpha_{I_{sc}} (T_{cell} - T_{stc}) \quad (11)$$

205

206

$$207 \quad V_{mp}^{corr} = V_{mp} + N_s a V_T \ln \left(\frac{G}{G_0} \right) + \beta_{V_{oc}} (T_{cell} - T_{stc}) \quad (12)$$

208

209
210
211
212

Where N_s is the number of series-connected cells in the module, a is the ideality factor and $\beta_{V_{oc}}$ is the temperature coefficient for the open circuit voltage.

213
214
215

3. Assessment of modeling I-V curves at indoor standard test conditions

216
217
218
219
220
221
222
223
224
225
226
227
228
229

The evaluation of the modeling was performed by collecting and using experimental I-V curves for several modules measured at Ciemat PV Lab in previous projects and tests. Thus, indoor measurements of I-V curves of modules of several technologies had been performed at Ciemat in a large-area solar simulator type one-pulse-flash (pulse times of 10 ms) and class AAA (IEC 60 904-9). All measurements were performed at temperature and irradiance values nearly to STC ($1000 \pm 5 \text{ W/m}^2$ and $25 \pm 2^\circ \text{ C}$). Temperature and irradiance corrections were negligible because the test values were nearly STC ones. In addition, no spectral corrections were performed. Table 1 shows the manufacturer parameters for six different modules of monocrystalline silicon (m-Si), multicrystalline silicon (mc-Si), amorphous silicon (a-Si), cadmium telluride (CdTe) and copper indium selenide (CIS), measured in the solar simulator.

Table 1. Manufacturer data for different technology modules.

| Module Technology | N_s | Power (W) | I_{mp} (A) | V_{mp} (V) | I_{sc} (A) | V_{oc} (V) |
|-------------------|-------|-----------|--------------|--------------|--------------|--------------|
| CdTe | 154 | 80 | 1.58 | 50.7 | 1.76 | 61.7 |
| CIS | 56 | 80 | 2.29 | 35.0 | 2.50 | 44.0 |
| m-Si Back-Contact | 72 | 238 | 5.88 | 40.5 | 6.25 | 48.5 |
| a-Si | 159 | 85 | 0.87 | 97.7 | 1.10 | 136.5 |
| mc-Si Atersa | 72 | 180 | 5.00 | 36.1 | 5.20 | 44.3 |
| mc-Si Yingly | 60 | 265 | 8.70 | 30.5 | 9.18 | 37.8 |

230
231
232
233
234
235
236
237
238
239
240
241
242
243
244
245
246
247
248
249
250

For each module, the procedure detailed in section 2 has been followed to compute the I-V curve at STC from the manufacturer's parameter values. The five parameters estimated by the model are listed in Table 2 for the six PV modules. Figure 1 shows the I-V curve calculated by the model from the manufacturer initial parameters compared to the experimental curve measured at the flash simulator. The results are very accurate in the Si modules and worse in the case of thin film modules. For CdTe and CIS modules the modeled I-V curves were very close to the experimental ones, but their open circuit voltages were underestimated. In the case of the a-Si module, significant differences were found due to large differences in the initial parameters used. It has to be noticed that the measured I-V curve showed in figure 3 is the measurement of the module when delivered, previous to the initial degradation and stabilization of a-Si that is normally taken into account in manufacturer module parameters (Kroposki, 1997; Sanchez et al., 2014). However, in order to ensure that the differences were not attributed to the algorithm it was proven that the model reproduced perfectly the experimental I-V curve of a-Si when measured parameters were used: $I_{mp} = 1.008 \text{ A}$, $V_{mp} = 115.79 \text{ V}$, $I_{sc} = 1.16 \text{ A}$ and $V_{oc} = 145.67 \text{ V}$. These parameters have been measured for the a-Si module experimentally with flash simulator and showed important differences to the manufacturer data listed in table 1. In case of using these measured parameters instead of those of table 1 the I-V curve measured is perfectly reproduced by the model. It must be pointed out that this difference cannot be attributed to the manufacturer since the module

251 was measured in Ciemat PV lab before illumination and thus without taking into account the
 252 natural light-induced degradation effect (Staebler-Wronski effect) which is usually accounted
 253 in the manufacturer data.

254

255 Table 2. Five parameters estimated by modeling and solving the single diode equation.

256

257

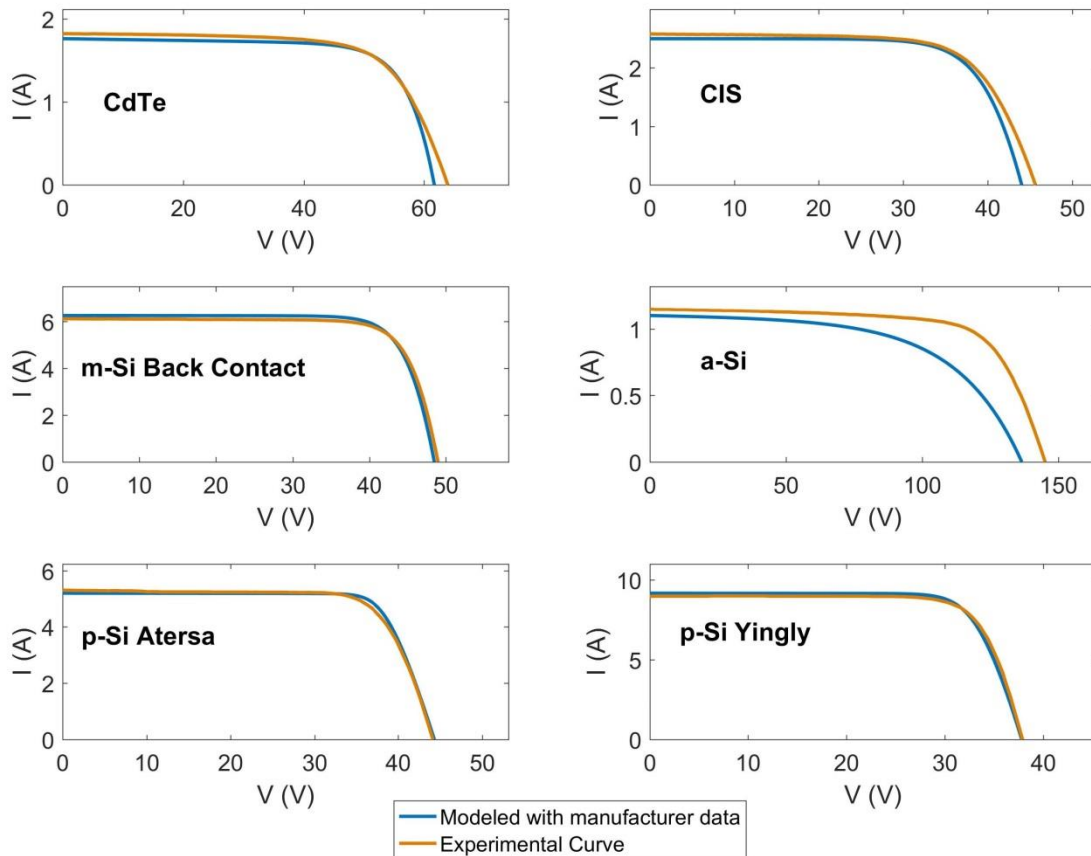
| Module Technology | a | I_L (A) | I_0 (A) | R_S (Ω) | R_{sh} (Ω) |
|-------------------|------|-----------|-----------|--------------------|-----------------------|
| CdTe | 1.05 | 1.76 | 6.012e-7 | 0.118 | 929.5 |
| CIS | 2.1 | 2.50 | 1.182e-6 | 0.639 | 8.644e+3 |
| m-Si Back-Contact | 1.3 | 6.25 | 1.087e-8 | 0.192 | 3.513e+3 |
| a-Si | 5.7 | 1.1 | 0.003 | 0.047 | 3.298e+3 |
| p-Si Atersa | 0.65 | 5.20 | 5.181e-16 | 0.831 | 2.880e+3 |
| p-Si Yingly | 0.95 | 9.18 | 5.652e-11 | 0.336 | 1.605e+3 |

258

259

260

261



262

263

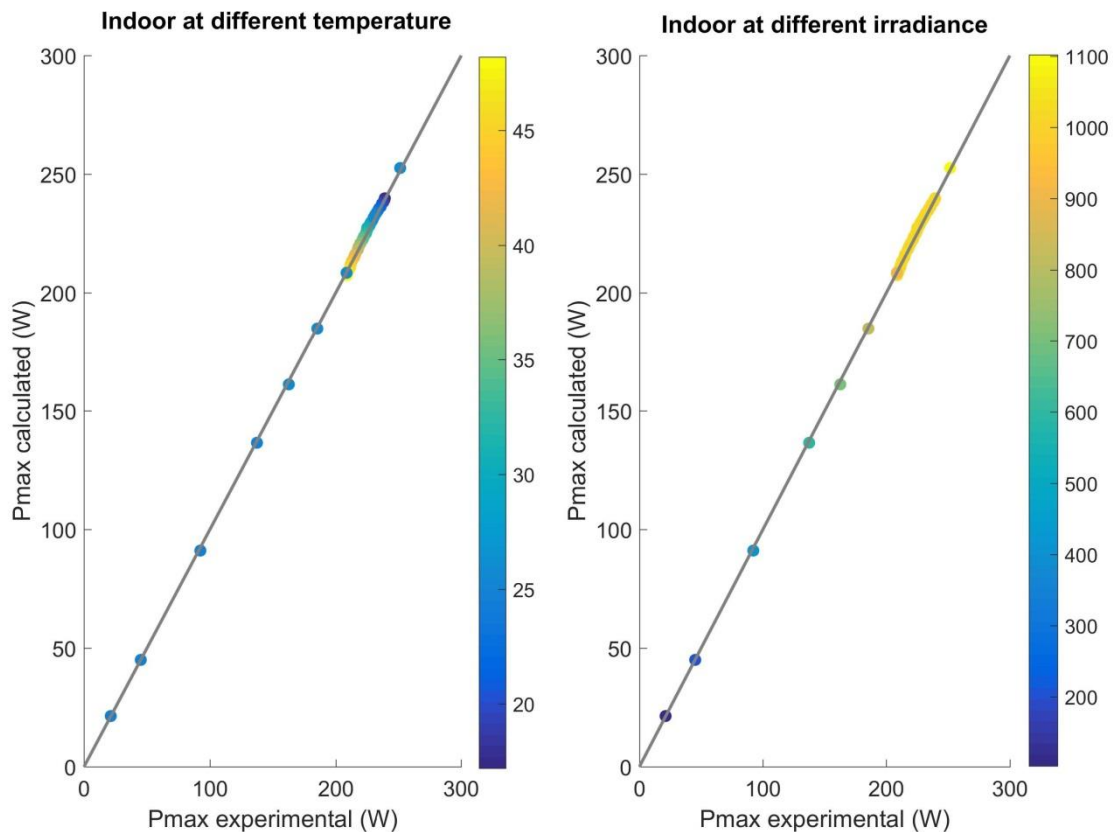
264 Fig. 3. Comparison of the I-V curves modeled and measured at STC.

265

266

267 In order to compare the methodology for different temperature and irradiance at indoor
 268 conditions, several measurements were performed at CIEMAT with the solar simulator for a
 269 mc-Si module of Yingly Solar. Module temperature was ranged from 20 °C to 44 °C and solar
 270 irradiance from 200 to 950 W m⁻². The diode equation was solved using the procedure

271 described in section 2, iterating the ideality diode factor and solving the equation by the
 272 Lambert-W function for estimating the five parameters at STC. Then the five parameters were
 273 extrapolated to the temperature and irradiance conditions by the equations (4-8), here
 274 referred to as first procedure. At each temperature and irradiance condition the I-V curve as
 275 well as the maximum power were estimated. Figure 4 shows a scatter plot of the maximum
 276 power at different temperatures and solar irradiances with excellent agreement with the
 277 maximum power extracted from the experimental I-V curve (the root mean squared error
 278 between modeled and experimental maximum power was 0.45 W, representing 0.22%). In
 279 addition, in the case of the second procedure for extrapolating to temperature and irradiance
 280 conditions beyond STC, equations (9-12) have been used to extrapolate the short circuit
 281 current, open circuit voltage and the maximum power according to the temperature and solar
 282 irradiance established in the simulator, and for every new situation the single diode model was
 283 solved using the procedure described in this work. The resulted new I-V curves were nearly
 284 identical to those obtained by correcting the five parameters. The root mean error of the
 285 maximum power from the I-V curves using the second approach was 0.46 W, i.e. practically the
 286 same than the first approach.
 287
 288
 289
 290
 291



292
 293
 294
 295
 296

Fig. 4. Scatter plots of maximum power at different indoor temperature and irradiance conditions for a p-Si module (Yingly 230-P).

297 **4. I-V curve at outdoor conditions**
 298

299 In order to explore the approach for modeling the IV curve in outdoor conditions three
 300 modules have been monitored during one day (3rd September 2018). The modules tested were
 301 all of m-Si technology south oriented and with a tilt angle of 30°. The experimental IV curve is
 302 measured around every 8 minutes using I-V-curve measuring device PVPM2540C
 303 manufactured by PVE Photovoltaik Engineering. For monitoring the I-V curves and other
 304 parameters in a continuous manner, a specific commutation system was mounted for driving
 305 the signal sequentially to the every module after each measurement. Irradiance at the plane of
 306 the array was measured with a calibrated solar cell, and the temperature of each module was
 307 measured with a thermocouple on the back side. Manufacturer data for each module are
 308 listed in table 3. Figure 5 illustrates the plane of array (POA) irradiance and the module
 309 temperature measured for the Photowatt module during a whole day.

310

311

312

313 Table 3. Manufacturer data for three monitored m-Si modules, with the same number of cells
 314 in series.

315

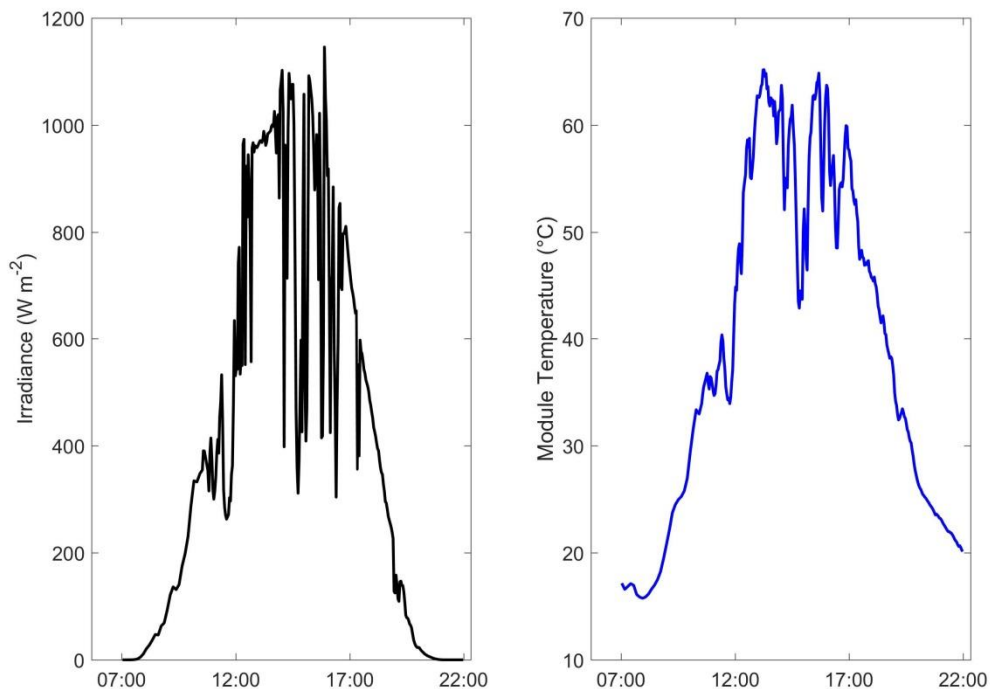
| Module | N_s | Power (W) | I_{mp} (A) | V_{mp} (V) | I_{sc} (A) | V_{oc} (V) |
|------------------|-------|-----------|--------------|--------------|--------------|--------------|
| Panasonic HIT | 72 | 225 | 5.21 | 43.2 | 5.54 | 52.4 |
| Photowatt PW1650 | 72 | 165 | 4.80 | 34.3 | 5.10 | 43.2 |
| EGNG EGM180 | 72 | 180 | 5.12 | 35.1 | 5.54 | 44.3 |

316

317

318

319



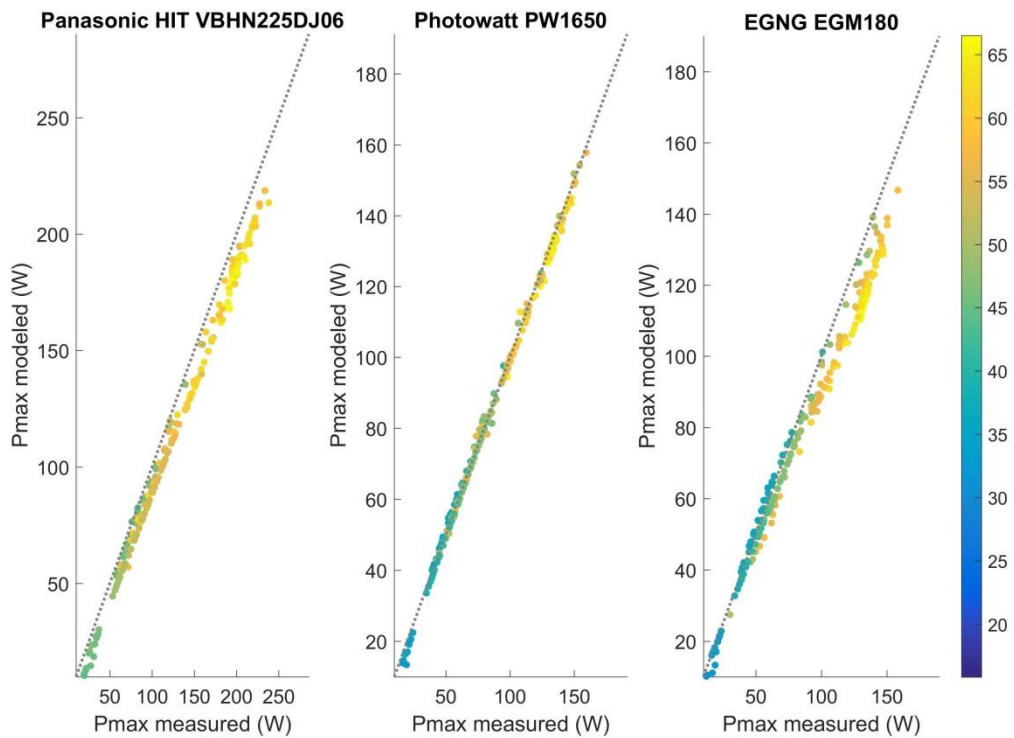
320

321 Fig. 5. POA irradiance and module temperature recorded for a Photowatt module on 3th
 322 September 2018.

323

324

325 For each module and timestamp the POA irradiance and the module temperature have been
 326 used to derive the corresponding I-V curve at outdoor conditions using the two procedures
 327 described in this paper: modeling the five parameters from the simplified diode equation at
 328 STC from the manufacturer data and extrapolating the parameters to outdoor conditions, and
 329 extrapolating the manufacturer data to outdoor conditions and solving the simplified diode
 330 equation for the new extrapolated initial parameters. Instead of comparing the experimental
 331 and calculated I-V curves each other the maximum power has been obtained from the I-V
 332 experimental and modeled curves for the comparison. Figure 6 and 7 shows the scatter plots
 333 of the maximum power obtained by the first and the second procedure, respectively.
 334
 335
 336



337
 338
 339
 340
 341

Fig. 6. Scatter plots of maximum power points taken from the I-V curves of three m-Si modules modeled by the first procedure.

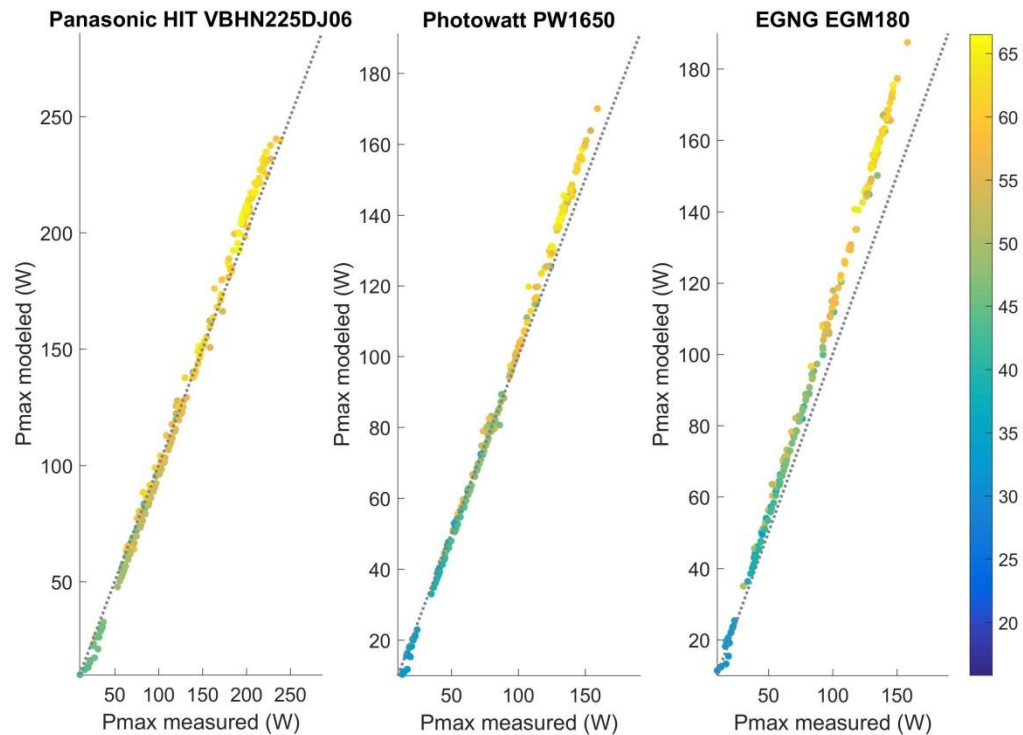


Fig. 7. Scatter plots of maximum power points taken from the I-V curves of three m-Si modules modeled by the second procedure.

The results for outdoor conditions are good in general terms; however they show some differences among the different modules. The highest accuracy was found for the case of Photowatt module. Additional differences were also found in the results of extrapolating to outdoor conditions with first and second procedure described in the methodology section. Since the methodology has proven to be very accurate at indoor conditions, where module temperature and solar irradiance were accurately controlled, the differences observed in the outdoor conditions tests could be attributed to the impact of the uncertainty in the input parameters on the modeled I-V curve. In outdoor conditions the uncertainty of the input parameters can be divided in two groups: the uncertainty in the manufacturer datasheet parameters and the uncertainty in the environment measurements (particularly the module temperature and the solar irradiance at outdoor conditions). In addition, other sources of uncertainty can arise in the outdoor conditions such as soiling, angular and spectral effects, whose impact is difficult to be determined when input and boundary parameters have an unknown level of uncertainty.

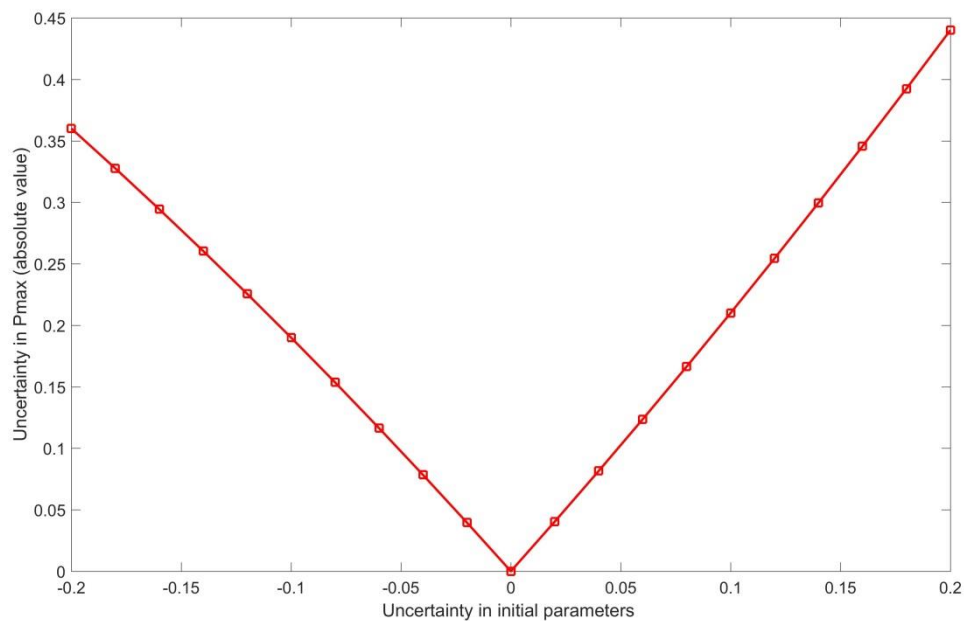
In order to investigate the impact of the uncertainty in the manufacturer datasheet parameters in the methodology for modeling the I-V curve, sensitivity analysis were performed using the proposed model with the datasheet parameters of the Photowatt module. Assuming that the manufacturer data in table 3 for the Photowatt module are perfectly accurate the sensitivity analysis of the model was performed by perturbing artificially all the input parameters at different levels of uncertainty. For a range of 0-20% of uncertainty (i.e. from 20% underestimation to 20% overestimation in all the input parameters) the methodology was followed to compute I-V curve at STC conditions. Figure 8 shows the uncertainty (in terms of relative absolute deviation) in the maximum power of the modeled I-V curve as a function of the uncertainty in the input parameters, in other words it shows the sensitivity of the model to

373 the uncertainty of the input. The results show that the errors have a linear propagation in the
 374 model for computing the I-V curve. However error in the maximum power increases slightly for
 375 larger errors in the input parameters. Thus, a 20% of overestimation in the input parameters
 376 resulted in near a 45% of overestimation in the maximum power, and conversely an
 377 underestimation of 20% in the input parameters resulted in underestimations of around 35%
 378 of the maximum power.

379

380 The extrapolation of the uncertainty due to inaccurate values of the manufacturer datasheet
 381 parameters to different temperature and irradiance conditions is complex because the
 382 different sources of uncertainty cannot be easily separated, at least in the experimental
 383 conditions available to the outdoor tests in this work. Therefore, a new sensitivity analysis was
 384 done for the case of very well controlled temperature and irradiance conditions. This new
 385 study consisted on using the flash I-V curves measured at different and controlled temperature
 386 and irradiance values for the Yingly 230-P module. Since the results of modeling I-V curve at
 387 different temperature and irradiance for this module were very accurate (Figure 4), it was
 388 assumed that the manufacturer data were perfectly accurate and the I-V curves were modeled
 389 again increasing and decreasing the input parameters by a 10%. Figure 9 shows the scatter
 390 plots for the maximum power obtained from the computed I-V curves.

391



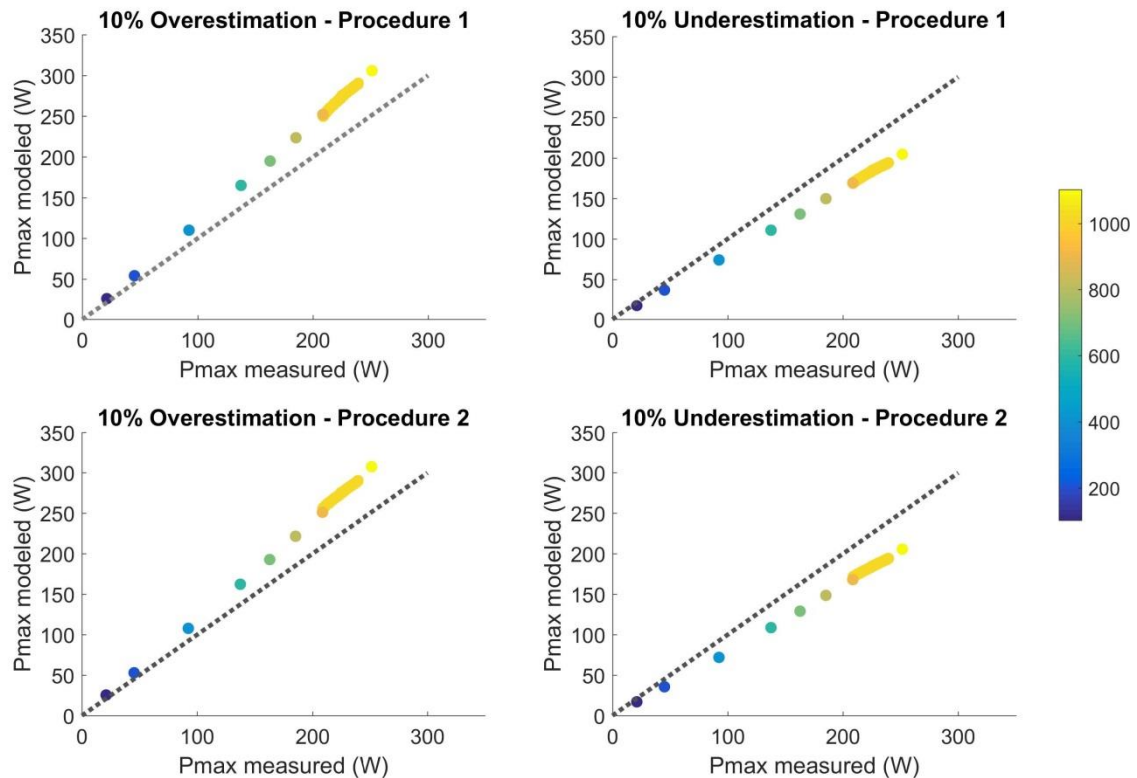
392

393

394

395 Fig. 8. Propagation of the uncertainty in the input parameters

396



397
398

399 Fig. 9. Sensitivity in the modeled maximum power to irradiance and temperature for a 10% of
400 uncertainty in the input parameters for Photowatt module.

401
402
403

404 As expected the overestimation in the input parameters of the model resulted in
405 overestimation of the maximum power and, conversely, underestimation in the input resulted
406 in underestimating the maximum power. Moreover, the error in the estimated maximum
407 power or in the estimated I-V curves increases with the irradiance and with the module
408 temperature. It should be also emphasize that the differences between using the first or
409 second procedure for extrapolating the I-V curves to temperatures and irradiances beyond STC
410 were practically negligible.

411

412 5. Conclusions

413

414 Modeling accurately the I-V curve of a photovoltaic module from the basic parameters
415 appearing in the manufacturer's datasheet can be of high interest in many applications. In this
416 work a fast and straight method is presented for solving the single diode equivalent circuit
417 equation to deriving the five parameters. The methodology is based on a previous proposal in
418 the literature where the Lambert-W function was used to obtain four parameters under the
419 prior knowledge of the ideality factor of the diode. In this work an iterative procedure is
420 proposed in combination with the aforementioned simple method to obtain the five
421 parameters fast, accurately and in a straight way.

422

423 The methodology presented here has been assessed with experimental data available from
424 previous projects and tests performed with different modules at Ciemat's PV Lab. The

425 comparison with measurements made with a flash solar simulator showed rather accurate
 426 results. In addition, for very well controlled conditions of module temperature and solar
 427 irradiance at indoor measurements the methodology was very accurate in computing the I-V
 428 characteristic curve at STC and at different temperature and irradiance conditions. The
 429 evaluation of indoor conditions has proven the robustness and accuracy of the methodology
 430 proposed. Differences became slightly larger for outdoor tests, particularly for higher
 431 temperatures and irradiance. In this regard a sensitivity analysis has been performed to
 432 investigate the sources and propagation of the uncertainties. In particular, it might be of high
 433 interest to know the sensitivity to the uncertainty in the input parameters The results have
 434 shown the impact of the uncertainty in the manufacturer's datasheet, which might be
 435 important, particularly in conditions of high module temperature or irradiance.

436
 437 In conclusion, the methodology presented in this work allows the accurate computation of the
 438 I-V curve of a photovoltaic module from manufacturer's datasheet at STC and other conditions
 439 of temperature and irradiance. The model presented is fast and very easy to be implemented
 440 in any tool for modeling requiring only a few equations and small number of iterations.
 441 Nevertheless, the accuracy is conditioned by the uncertainty of the input parameters used.

442

443 **Acknowledgements**

444 The authors would like to thank the PVCastSOIL Project (ENE2017-469 83790-C3-1, 2 and 3),
 445 which is funded by the Ministerio de Economía y Competitividad (MINECO), and co-financed by
 446 the European Regional Development Fund. In addition, this work has been partially funded by
 447 the Ministerio de Economía y Competitividad (MINECO), Acciones de Programación Conjunta
 448 Internacional, Project PCIN-2015-027, according to the First ERANETMED Joint Transnational
 449 Call (7th EU RTD Framework Programme).

450

451 **References**

452

453 Andrews, R.W., Stein, J.S., Hansen, C., Riley, D., 2014. Introduction to the open source pvlb for
 454 python photovoltaic system modelling package, in: 40th IEEE Photovoltaic Specialist
 455 Conference.

456 Ayodele, T.R., Ogunjuyigbe, A.S.O., Ekoh, E.E., 2016. Evaluation of numerical algorithms used in
 457 extracting the parameters of a single-diode photovoltaic model. *Sustainable Energy*
 458 *Technologies and Assessments* 13, 51–59. doi:10.1016/j.seta.2015.11.003

459 Celik, A.N., Acikgoz, N., 2007. Modelling and experimental verification of the operating current
 460 of mono-crystalline photovoltaic modules using four- and five-parameter models. *Applied*
 461 *Energy* 84, 1–15. doi:10.1016/j.apenergy.2006.04.007

462 Ciulla, G., Lo Brano, V., Di Dio, V., Cipriani, G., 2014. A comparison of different one-diode
 463 models for the representation of I–V characteristic of a PV cell. *Renewable and*
 464 *Sustainable Energy Reviews* 32, 684–696. doi:10.1016/j.rser.2014.01.027

465 Cubas, J., Pindado, S., De Manuel, C., 2014. Explicit expressions for solar panel equivalent
 466 circuit parameters based on analytical formulation and the lambert W-function. *Energies*
 467 7, 4098–4115. doi:10.3390/en7074098

468 De Soto, W., Klein, S.A., Beckman, W.A., 2004. Improvement and validation of a model for
 469 photovoltaic array performance. MS Mechanical Engineering Thesis. University of
 470 Wisconsin-Madison.

- 471 De Soto, W., Klein, S.A., Beckman, W.A., 2006. Improvement and validation of a model for
472 photovoltaic array performance. *Solar Energy* 80, 78–88.
473 doi:10.1016/j.solener.2005.06.010
- 474 Dobos, A.P., 2012. An Improved Coefficient Calculator for the California Energy Commission 6
475 Parameter Photovoltaic Module Model. *Journal of Solar Energy Engineering* 134, 021011.
476 doi:10.1115/1.4005759
- 477 Dobos, A.P., 2014. PVWatts Version 5 Manual. Technical Report NREL/TP-6A20-62641,
478 Golden,USA.
- 479 Et-Torabi, K., Nassar-Eddine, I., Obbadi, A., Errami, Y., Rmailly, R., Sahnoun, S., El, A., Agunaou,
480 M., 2017. Parameters estimation of the single and double diode photovoltaic models
481 using a Gaussian Seidel algorithm and analytical method: A comparative study.
482 doi:10.1016/j.enconman.2017.06.064
- 483 Ghani, F., Rosengarten, G., Duke, M., Carson, J.K., 2014. The numerical calculation of single-
484 diode solar-cell modelling parameters. *Renewable Energy* 72, 105–112.
485 doi:10.1016/j.renene.2014.06.035
- 486 Green, M.A., 1981. *Solar Cells: Operating Principles, Technology, and System Applications*.
487 Prentice Hall.
- 488 Gurupira, T., Rix, A.J., 2017. PV Simulation Software Comparisons : Pvsyst , Nrel Sam and Pvlb,
489 in: SAUPEC 2017.
- 490 Holmgren, W.F., Andrews, R.W., Lorenzo, A.T., Stein, J.S., 2015. PVLIB Python 2015, in: 42nd
491 Photovoltaic Specialists Conference.
- 492 IEA-PVPS, 2018. Trends 2018 in Photovoltaics Applications, Report IEA PVPS T1-34:2018.
- 493 Jain, A., 2004. Exact analytical solutions of the parameters of real solar cells using Lambert W-
494 function. *Solar Energy Materials and Solar Cells* 81, 269–277.
495 doi:10.1016/j.solmat.2003.11.018
- 496 Kazakova, S.G., Pisanova, E.S., Angelopoulos, A., Fildisis, T., 2010. Some Applications of the
497 Lambert W-function to Theoretical Physics Education, in: AIP Conference Proceedings
498 1203. pp. 1354–1359. doi:10.1063/1.3322371
- 499 Kessaissia, F.Z., Zegaoui, A., Arab, A.H., Loukarfi, L., Aillerie, M., 2015. Comparison of Two PV
500 Modules Technologies Using Analytical and Experimental Methods. *Energy Procedia* 74,
501 389–397. doi:10.1016/j.egypro.2015.07.635
- 502 Khezzar, R., Zereg, M., Khezzar, A., 2014. Modeling improvement of the four parameter model
503 for photovoltaic modules. *Solar Energy* 110, 452–462.
504 doi:10.1016/J.SOLENER.2014.09.039
- 505 King, B.H., Hansen, C.W., Riley, D., Robinson, C.D., Pratt, L., 2016. Procedure to Determine
506 Coefficients for the Sandia Array Performance Model (SAPM). Sandia Report, SAND2016-
507 5284.
- 508 King, D.L., Boyson, W.E., Kratochvill, J.A., 2004. Photovoltaic Array Performance Model. Sandia
509 Report. doi:10.2172/919131
- 510 Kroposki, B., 1997. Can the Staebler-Wronski Effect Account for the Long-Term Performance of

- 511 a-Si PV Arrays ? 313. doi:10.1063/1.52849
- 512 Mares, O., Paulescu, M., Badescu, V., 2015a. A simple but accurate procedure for solving the
513 five-parameter model. *Energy Conversion and Management* 105, 139–148.
514 doi:10.1016/j.enconman.2015.07.046
- 515 Mares, O., Paulescu, M., Badescu, V., 2015b. A simple but accurate procedure for solving the
516 five-parameter model. *Energy Conversion and Management* 105, 139–148.
517 doi:10.1016/j.enconman.2015.07.046
- 518 Nassar-Eddine, I., Obbadi, A., Errami, Y., El Fajri, A., Agunaou, M., 2016. Parameter estimation
519 of photovoltaic modules using iterative method and the Lambert W function: A
520 comparative study. *Energy Conversion and Management* 119, 37–48.
521 doi:10.1016/j.enconman.2016.04.030
- 522 Peng, J., Lu, L., Yang, H., Ma, T., 2015. Validation of the Sandia model with indoor and outdoor
523 measurements for semi-transparent amorphous silicon PV modules. *Renewable Energy*
524 80, 316–323. doi:10.1016/j.renene.2015.02.017
- 525 Rasool, F., Drieberg, M., Badruddin, N., Singh, B., Singh, M., 2017. PV panel modeling with
526 improved parameter extraction technique. *Solar Energy* 153, 519–530.
527 doi:10.1016/j.solener.2017.05.078
- 528 Rhouma, M.B.H., Gastli, A., Ben Brahim, L., Touati, F., Benammar, M., 2017. A simple method
529 for extracting the parameters of the PV cell single-diode model. *Renewable Energy* 113,
530 885–894. doi:10.1016/j.renene.2017.06.064
- 531 Sanchez, E., Izard, J., Dominguez, M., 2014. Experimental Study of Light Induced Degradation in
532 a-Si:H Thin Film Modules under different climate conditions. 27th European Photovoltaic
533 Solar Energy Conference 651–653. doi:10.4229/27thEUPVSEC2012-3DV.1.12
- 534 Stein, J.S., Farnung, B., 2017. PV Performance Modeling Methods and Practices Results from
535 the 4th PV Performance Modeling Collaborative Workshop. IEA PVPS Task 13, Subtask 2
536 Report IEA-PVPS T13-06:2017.
- 537 Stein, J.S., Hansen, C.W., King, B.H., Sutterlueti, J., Ransome, S., 2013. Outdoor PV Performance
538 Evaluation of Three Different models: Single-diode SAPM and Loss Factor Model, in:
539 September 30 - October 4, P. (Ed.), 28th European Photovoltaic Solar Energy Conference.
- 540 Sudhakar Babu, T., Prasanth Ram, J., Sangeetha, K., Laudani, A., Rajasekar, N., 2016. Parameter
541 extraction of two diode solar PV model using Fireworks algorithm. *Solar Energy* 140, 265–
542 276. doi:10.1016/j.solener.2016.10.044
- 543 Valluri, S.R., Jeffrey, D.J., Corless, R.M., Valluri, S.R., Corless, R.M., Some Applications, D.J.J.",
544 Jeffrey, D.J., 2000. Some applications of the Lambert W function to physics, *Can. J.*
545 *Physics*.
- 546 Veberič, D., 2012. Lambert W function for applications in physics. *Computer Physics*
547 *Communications* 183, 2622–2628. doi:10.1016/J.CPC.2012.07.008
- 548
- 549